Progress In Electromagnetics Research C, Vol. 126, 13–22, 2022

A Circular Array with Improved Focusing Properties

Mohammed Z. Mohammed Fwzi and Khalil H. Sayidmarie*

Abstract—A concentric circular array consisting of two rings is proposed to focus the radiated field at a point in the near-field zone. In the proposed two-ring array, the radius of the outer ring was chosen so that the radiated fields from all elements on the two rings add constructively at the focal point, thus no phase shifter is needed in this design. The N elements of the inner ring are uniformly excited in unity amplitude and zero phase, while the M elements on the outer ring are excited uniformly in phase, and given uniform magnitude excitations of N/M. Therefore, two deep nulls are achieved on both sides of the focus to enhance the focal width. The focusing properties are investigated by exploring the array parameters, such as variation of the focused field along the normal to the array, field distribution on the focal plane, and depth of field (size of the focal spot). Computer simulations using the MATLAB environment are performed by point source radiators. For verification, the array was simulated using the CST microwave studio, and the obtained results showed good agreement. The array is useful for hyperthermia and imaging applications.

1. INTRODUCTION

Antenna is one of the important parts of wireless communication systems, where it is usually used in the far-field region. However, there are other applications where the antenna is required to radiate or receive an electromagnetic field that is concentrated in a certain region near the antenna. The antenna in this case is called a focused antenna, where the contributions of all elements add constructively at the focal point, and destructively elsewhere. The focusing of electromagnetic radiation has attracted continued interest in the last few decades, and diverse applications have been described. One of the applications is non-contact sensing by electromagnetic radiation, where a confined focused beam is used for industrial sensing [1] and ground penetration radar applications [2]. In medical applications, the focused antennas have been used in local hyperthermia, where localizing microwave power is used for tumor irradiation [3–5]. Various techniques have been used to achieve a focused beam in the near field at microwave frequency bands. Many of the technologies used for conventional unfocused antennas have been revised to implement near-field focused antennas [6].

The phased arrays are favorable in the applications of focused antennas as they offer flexibility and many degrees of freedom to the designers. Therefore, designers have used the geometry of the array, array size, amplitude, and phase excitations of the array elements to design focused arrays that meet the desired performance. To treat local hyperthermia, three array configurations were proposed to concentrate the radiation at a specific point [7]. The elements of the arrays were placed in a cross, rectangular ring, and the conventional lattice, and the focusing properties of the three array geometries were compared. The focusing properties of six different array configurations in the form of a square, square with interlaced elements, square ring, cross (+) shape, cross (X) shape, and square ring plus diagonals shape arrays were investigated, and their performances were compared in [8]. The compared performance parameters were field distribution in the focal region, size of the focal spot, depth of field,

Received 8 August 2022, Accepted 11 October 2022, Scheduled 25 October 2022
* Corresponding author: Khalil Hassan Sayidmarie (kh.sayidmarie@gmail.com).
The authors are with the Department of Communication Engineering, College of Electronics Engineering, Ninevah University, Mosul, Iraq.

level of the field at the focal point, and sidelobe structure. A printed square array antenna was used to focus the beam in the near field region, where the field radiated by the 16×16 elements of the array should be the sum at the focus. The array elements were designed to provide a dual-polarization, and the array has two focal spots [9].

A multi-panel focused antenna that is different from traditional planar arrays was proposed in [10]. The focused sub-arrays were arranged concentrically on cylindrical boundaries. Systematic numerical analysis was done to control the shape of the focal spot depending on parameters such as the main geometrical structure, the number of subarrays, the focal spot location of each subarray, and the radius of the circle on which the subarrays are arranged [10]. A multilayer, near-field focused array antenna using the substrate integrated waveguide (SIW) technology to achieve variable focus was presented in [11]. Metallic circular holes, which are fed by SIW feeding network, operate as both phase shifters and radiating elements. By changing the thickness of the hole layer, the antenna with the same feeding network can be adjusted to change its focal point. The 8×8 elements focused array achieved a side-lobe level of less than -18 dB in a prototype operating at 35 GHz [11].

In square-shaped arrays, the phase of the elements' excitations has to be precisely adjusted so that proper focusing is obtained. Artificial neural networks were used to provide a set of weights for the elements in the array to focus the radiation on a specific point of the specific near field [12]. In microwave power transmission application, the focused transmitting array is designed with a tapered amplitude distribution to achieve maximum beam collection efficiency at the focal point. However, this needs a feeding network with an arbitrary power division ratio, which is complicated and costly in practical applications. In [13], a high transmission efficiency array with equal-ratio steps amplitude distribution was proposed.

The circular geometry was also investigated where the array elements are placed on a circle, and the focal point is either at any point in the plane of the circular array or along the normal to the array plane. An example of the first configuration is the focused microwave array where the elements are placed on a semicircle, and the focus is at the center of the circle [5, 14]. In such an arrangement, there is no need for the phase shifts in the excitations of the elements as their distances to the focal point are the same. With the use of phase shifters, the focus can be placed at the wanted point in the array plane as presented in [5] for thermotherapy applications. In [15], the design of a circular Vivaldi antenna array for ultra-wideband near-field radar imaging is presented. The focused array can also be designed such that the focal point is on the normal to the array. A circular array for RFID applications with simple implementation and a low side-lobe level compared to the square configuration was proposed in [16]. The potential to focus an electromagnetic field at a spot using metasurface holograms was presented in [17]. The proposed design employed cavity-backed radiating slots placed on a circle, which are covered by a metasurface layer. A near-field focused circular array antenna operating at 2.45 GHz was reported in [18]. The array has 16 rectangular dielectric resonator elements fed by coaxial feed and placed on two circles. By adjusting the radius of the circles, the antenna achieves a controllable focal distance. A numerical optimization method was proposed to achieve the near-field focusing of square arrays and circular arrays, using the frequency diversity array approach to adjust the initial amplitude and operating frequency [19]. Numerical methods and full-wave simulation were used to verify the design.

In this research, a circular antenna array is used as an alternative to the conventionally used rectangular arrays. The proposed array consists of elements placed on two concentric rings. The radius of the outer ring was chosen such that the distances from the elements on the outer rings to the focal point differ by one wavelength from those for the elements on the inner ring. Thus, the contributions of all elements add constructively at the focus, and consequently no phase shifter is needed. This is a considerable reduction as compared to the case of an $N \times N$-element square array where $N \times N/4$ phase shifters are required. Moreover, the elements on both rings are uniformly excited in amplitude and phase, while the elements on the outer ring are given smaller magnitude excitations such that each ring contributes equally to the field at the focal point. Therefore, a high peak is obtained at the focus that is accompanied by two adjacent deep nulls that enhance the focusing along the normal direction to the array. The paper is organized as follows. After an introduction and survey in Section 1, the circular array is discussed in Section 2. Section 3 explains the proposed two-ring array, and the results of the computer simulations are given in Section 4, which is followed by the drawn conclusions in Section 5.

2. ANALYSIS OF THE CIRCULAR ANTENNA ARRAY

One of the popular antenna array geometries is circular shape, where the elements of the array are placed on concentric rings. The radiation pattern of the circular array depends on the radius of the array, the number of rings in the array, the number of elements on each ring, as well as the magnitude and phase excitations of the elements. Consider N isotropic radiators uniformly placed on a circular ring of radius a, which is placed in the XY-plane. The origin of the coordinate system is located at the center of the array as shown in Fig. 1.

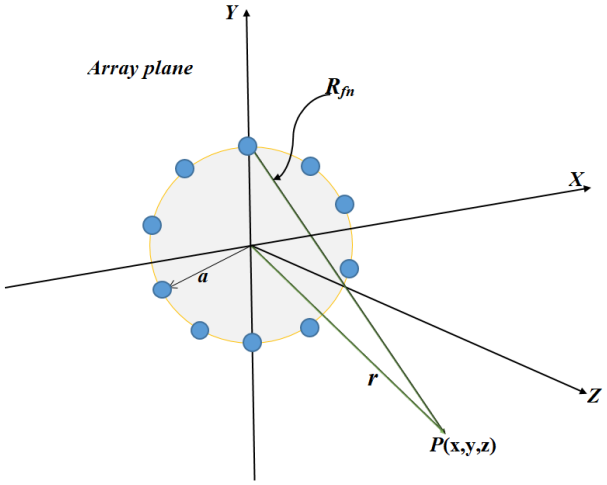

Figure 1. Geometry of a circular antenna array of N elements positioned on the XY-plane.

The total radiated field due to the N elements of the array at an observation point $P(x, y, z)$ in the near field of the array can be given by [8, 20]:

$$E_(x, y, z) = \sum_{n=1}^{N} I_n \frac{e^{-jkR_{fn}}}{R_{fn}} \tag{1}$$

where

$$\begin{aligned} R_{fn} &= \sqrt{[(x - x_n)^2 + (y - y_n)^2 + (z)^2]} \\ x_n &= a\cos(\phi_n) \\ y_n &= a\sin(\phi_n) \\ \phi_n &= 360n/N \end{aligned} \tag{2}$$

where k is the propagation constant, R_{fn} the distance from the nth element of the array to the observation point $P(x, y, z)$, and I_n the excitation of the nth element. When the observation point is assumed to be on the normal to the array, i.e., on the point $P(0, 0, z)$, and the N elements are uniformly excited, due to the symmetry of the array elements, the values of R_{fn} are all equal, and thus Eq. (1) reduces to:

$$E_1(0, 0, z) = \frac{Ne^{-jkR_{fn}}}{R_{fn}} \tag{3}$$

$$R_{fn} = \sqrt{(a^2 + z^2)} \tag{4}$$

This means that the electric field E_1 decays inversely with the distance of the observation point from the array center. The symmetry in the location of the elements leads to constructive addition of the radiations from the elements for all values of z. Therefore, to achieve a focus at a certain point $P(0, 0, z)$, some other elements' distances from the focal point vary in a different manner from those of the current ring. This difference in the distances causes constructive and destructive interferences that lead to the field focusing.

3. ANALYSIS OF THE TWO-RING FOCUSED CIRCULAR ARRAY

Figure 2 shows the geometry of the proposed circular array comprising two rings, and it is to be focused in the near field region at the point $P(0,0,F)$, on the normal to the array plane where F is the focal distance. The inner ring has N elements and radius a, while the outer ring has radius b and M elements. An expression for the near field of the focused array can be derived following the analysis in [8, 20] as

$$E(x,y,z) = \sum_{m=1}^{M}\sum_{n=1}^{N} C_{nm}\frac{e^{-jkR_{fnm}}}{R_{fnm}} \tag{5}$$

here $k = 2\pi/\lambda$ is the propagation constant, and R_{fnm} are magnitudes of the vectors shown in Fig. 2.

$$\begin{aligned} R_{fnm} &= \sqrt{[(x-x_{nm})^2 + (y-y_{nm})^2 + (z)^2]} \\ r_{nm} &= \sqrt{x_{nm}^2 + y_{nm}^2} \\ x_{nm} &= r_{nm}\cos(\phi_{nm}) \\ y_{nm} &= r_{nm}\sin(\phi_{nm}) \\ \phi_{nm} &= 360n/N, \quad n = 1,2,3,.....,N, \quad m = 1,2. \end{aligned}$$

The angular position of the nmth element on the ring is given by the angle ϕ_{nm}. The factor C_{nm} is the complex weighting of the nmth element, and it is given by:

$$C_{nm} = I_{nm}e^{j\Psi nm} \tag{6}$$

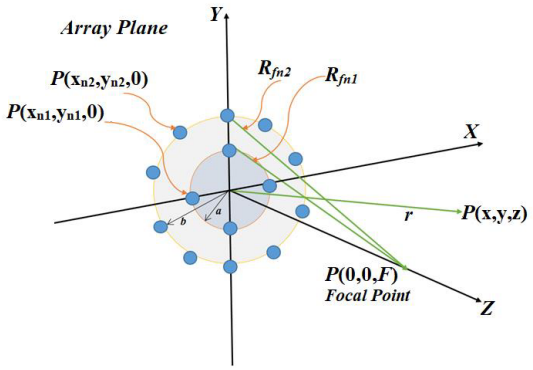

Figure 2. Geometry of the focused array of two concentric rings positioned in the XY-plane.

In the focused arrays, the excitations of the elements on the rings should be arranged such that the contributions of all the elements in one ring should add constructively to those due to the other ring at the focal point. This can be accomplished either by using a phase shifter or by proper choice of the radii of the two rings. In this proposed design, the radii of the two rings were chosen to fulfill the constructive addition of all the elements at the focal point, so that no phase shifter is needed. This can be a considerable achievement in comparison with the planar array which requires $N \times N/4$ phase shifters. As shown in Fig. 2, the distances R_{fn1} and R_{fn2} from the elements of the inner and outer rings respectively to the focal point $P(0,0,F)$ are:

$$R_{fn1} = \sqrt{(a^2 + F^2)} \tag{7}$$

$$R_{fn2} = \sqrt{(b^2 + F^2)} \tag{8}$$

where a and b are the radii of the inner and outer rings, respectively, and F is the focal distance. In the above equations, the array is assumed to be focused at the point $P(0,0,F)$. The difference between the path lengths R_{fn2} and R_{fn1} should be set to zero or multiple of wavelengths so that the contributions of the elements on the inner ring add constructively to those due to the outer ring. Since this difference

$(R_{fn2} - R_{fn1})$ cannot be set to zero without ring overlap, it was set to one wavelength to conserve the size of the array.

$$R_{fn2} = R_{fn1} + \lambda \tag{9}$$

Then the total field E_t due to the two rings is the sum of

$$E_t(x, y, z) = E_1(x, y, z) + E_2(x, y, z) \tag{10}$$

The proposed focused two-ring array was simulated in a MATLAB environment, and its performance was investigated by assessing the indicators such as field distributions around the focal plane, size of the focal spot or depth of field, level of the field at the focal point, and sidelobe structure.

4. COMPUTER SIMULATIONS

A general computer program was written in MATLAB environment to calculate the electric field distribution in the near field region of the array antenna. The radius of the inner ring was set at one wavelength, and the number of elements on the ring was assumed $N = 4$. The outer ring was assumed to have $M = 10$ elements; such an assumption is to keep almost equal distances between the array elements. The frequency of operation was assumed as 2.4 GHz, and the following analysis is applicable to other frequencies. The focal point was assumed at the normal to the array and located at $P(0, 0, F)$ where the focal distance is $F = 5\lambda$. The magnitude excitations of the elements on the inner ring were assumed at unity, while those for the outer ring were set equal to $N/M = 0.4$, so that the two rings contribute equally to the field at the focal point. The phase excitations of all the elements were made equal.

$$|C_{n1}| = 1, \quad |C_{n2}| = N/M|C_{n1}|, \quad \text{and } \psi_{nm} = 0 \tag{11}$$

Figure 3 shows the variation of the electric field at an observation point $p(0, 0, z)$ laying along the normal to the array. The inner array has four elements that are excited equally in magnitudes and phase ($I_{n1} = 1$, and $\psi_{n1} = 0$). The magnitude of the field $|E_1(0, 0, z)|$ due to the elements on the inner ring decays with the distance z as $1/z$ as predicted by Eqs. (3) and (4), while the angle of the field varies between $+ - \pi$ radians. It can be seen that there is no focus in the field, as all the elements remain at an equal distance from the observation point $P(0, 0, z)$ due to the circular symmetry, thus their radiated fields add constructively.

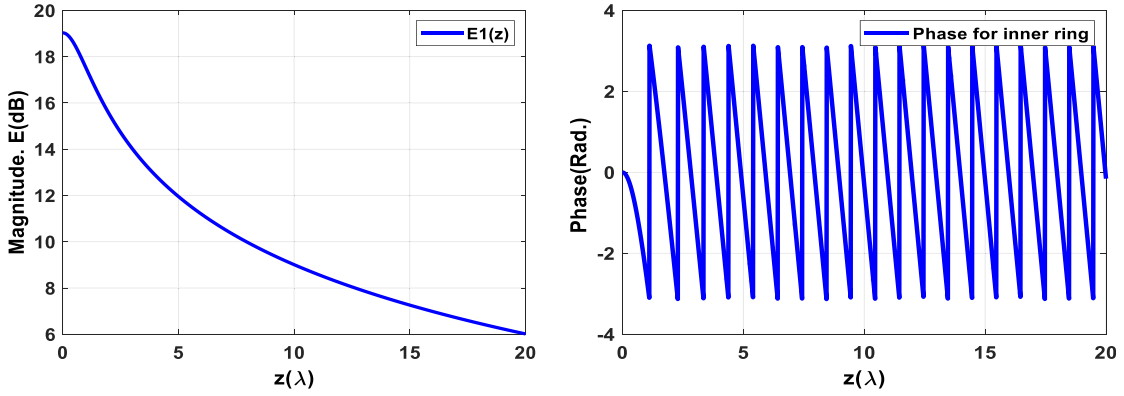

Figure 3. Variation of the magnitude and phase of the field $E_1(z)$ along the observation point $P(0, 0, z)$ when $N = 4$, and $F = 5\lambda$.

Now the field due to the outer ring is examined, and the radius of this ring was set at $b = 3.49\lambda$, according to Eqs. (7), (8), and (9). The outer ring array has ten elements that are excited equally in magnitudes (at 0.4) and zero phases. Fig. 4 shows the variation of the electric field on the observation point $P(0, 0, z)$ laying along the normal to the array. The magnitude of the field $|E_2(0, 0, z)|$ decays with the distance z as $1/z$ as predicted by Eqs. (3), and (4), while the angle of the field varies between

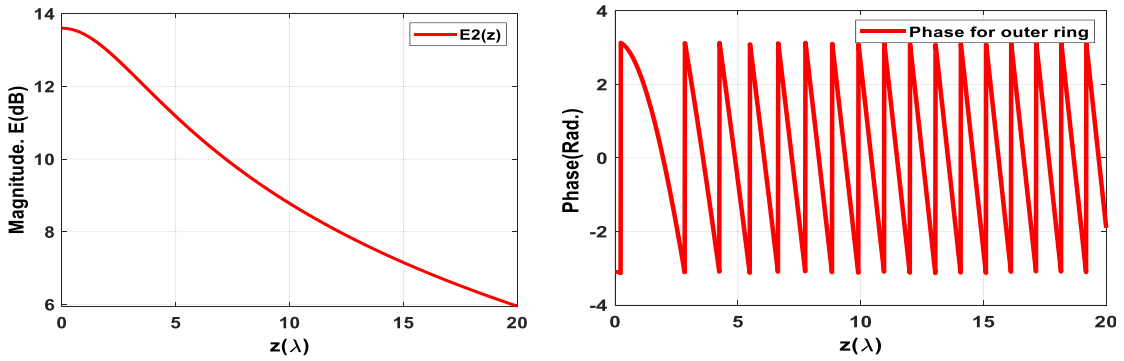

Figure 4. Variation of the magnitude and phase of the field $E_2(z)$ along the observation point $P(0,0,z)$ when $N = 10$, and $F = 5\lambda$.

$+-\pi$ radians. The variation of the field with distance follows a similar trend to that of the inner ring (Fig. 3), but the phase variation is slightly slower, which can be attributed to the larger distances R_{fn2} between the elements and the observation point. It can be seen that there is no focusing of the field, as all the elements remain at equal distances from the observation point $P(0,0,z)$ due to the circular symmetry.

Figure 5 shows the sum of the two radiated fields due to the two rings $E_t(x,y,z) = (E_1 + E_2)$ and how it varies at the observation point $P(0,0,z)$ along the normal to the array. Apart from the large values at the close proximity of the array elements, the field has a decaying trend in general. A focus indicated by a high peak at $z = 4.45\lambda$ can be seen, which is preceded by a sharp null and followed by another null, and a slowly decaying field. The 1st null is caused by the fact $z = 2.8\lambda$, and the value of E_1 is in antiphase to E_2, hence their sum $(E_1 + E_2)$ results in zero. The same condition of cancelation (2nd null) occurs at $z = 10.9\lambda$. The design has set the focus at $z = 5\lambda$, but the achieved focus has occurred at a slightly shorter distance of 4.45λ. The reason for this is that the decaying factor $(1/R_{fnm})$ leads to field reduction as z increases towards F. The depth of field is defined by the separation between the two points on either side of the peak where there is a drop by 3 dB, and it is found to be 3.8λ.

Figure 6 shows the variation of the phase of the fields due to the inner ring elements E_1 and the phase of the field E_2 due to the outer ring. It can be seen that the two phases are equal at $z = 5\lambda$, which confirms that the two contributions E_1 and E_2 add constructively at the focal point. Moreover, it can be seen that at $z = 2.8\lambda$ and $z = 10.9\lambda$, the fields E_1 and E_2 are in antiphase which explains the resulting nulls in the field variation.

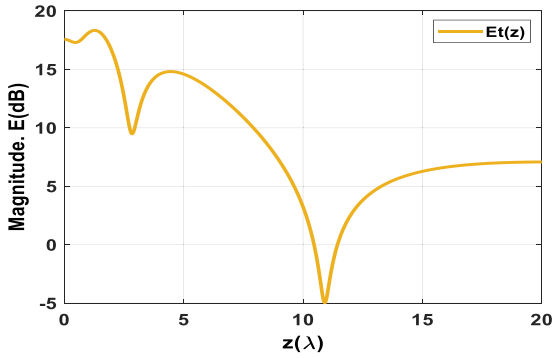

Figure 5. Variation of the magnitude of the total field $E_t(z)$ of the proposed array along the observation point $P(0,0,z)$ when $F = 5\lambda$, inner elements = 4, outer elements = 10.

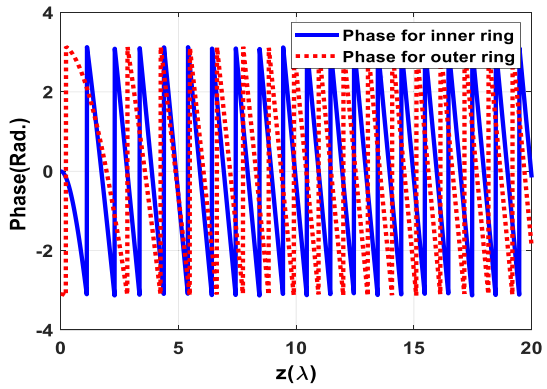

Figure 6. Variation of the phases of the fields $E_1(z)$ and $E_2(z)$ of the proposed array along the observation point $P(0,0,z)$ when $F = 5\lambda$, inner elements = 4, outer elements = 10.

A desirable feature of the focused arrays in medical applications is that the field values between the antenna and focal point are kept small so that the skin and tissue adjacent to the applicator (focused array) are not overheated. This property is very well met in this proposed design, as Fig. 5 shows that the field at the focal point is about 3 dB lower than that between the antenna and the focal point. Another useful property is that there is a null at $z = 10.5\lambda$ or at about $z = 2F$. In general, the field produced by a circular array varies along the normal to the array inversely, with no appearance of nulls. However, the proposed design has demonstrated that a null can be achieved along the normal axis, and its position can be easily chosen.

For further assessment of the field distribution around the focal point, the total field distribution across the XZ-plane is displayed in Fig. 7, which shows a localized focus along the normal to the array and the transversal direction along the X-axis. Fig. 8 shows the variation of the total field across the focal plane ($z = F$) which is parallel to the array plane. The focus is well defined and has circular symmetry, with low side lobes that are located symmetrically around the focus.

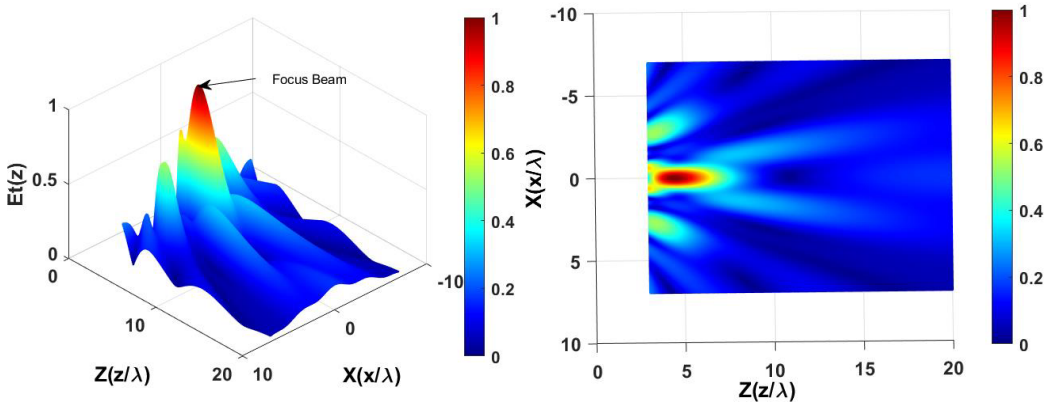

Figure 7. The total field variations across the XZ-plane for the proposed array.

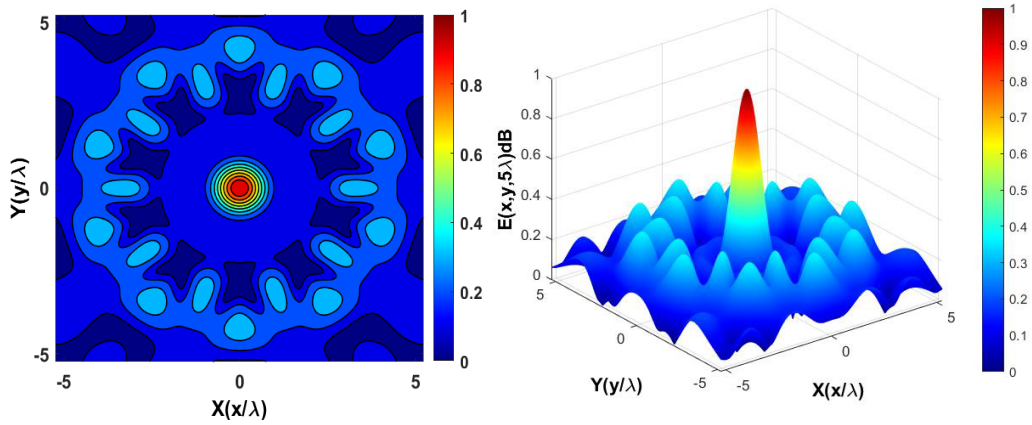

Figure 8. The total field variations across the focal plane at $z = F = 5\lambda$ for the proposed array.

The performance of the proposed array was assessed by investigating the influence of the focal distance. Fig. 9 shows the variation of the total field of the focused array along the normal to the array for various cases of focal distance F. The focus and two accompanying nulls are preserved for a wide range of focal distances. The depth of field varied as the focal distance was changed as shown in Fig. 10, which indicates an increasing depth of field (DOF) with the focal distance. It is noticed that the position of the achieved focus is short of the designed value of the focal distance. Fig. 11 shows how the shift in the position of the focal point from the desired design value varies with the value of the design focal distance.

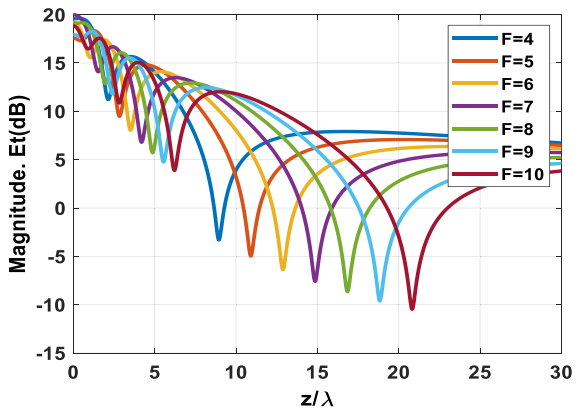

Figure 9. The total field variations along the normal axis to the proposed array for various values of the focal distance F.

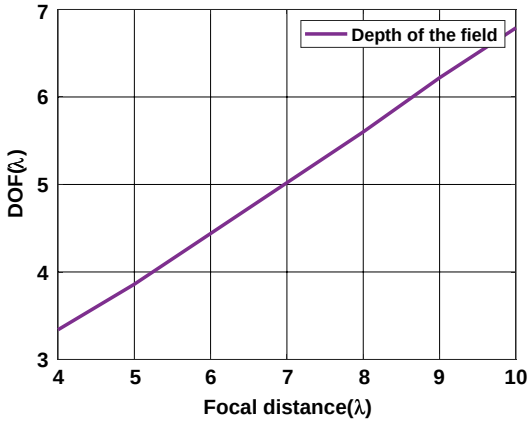

Figure 10. Variations of the depth of field with the focal distance for the proposed array.

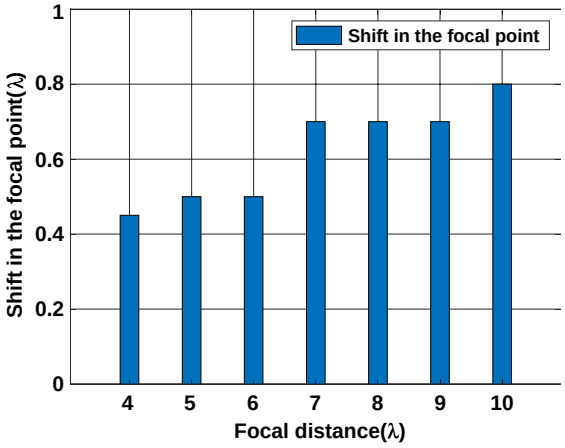

Figure 11. The variation of the shift in the position of the focus from the design value with the focal distance F.

5. FULL-WAVE SIMULATION

The proposed focused array was simulated using the Microwave Studio Suite to verify the theoretical analysis and the calculations obtained using the MATLAB program. The same number of elements and dimensions were used. However, in the CST simulations, instead of using point sources or isotropic elements, the array elements on the two rings were assumed as short dipole antennas, having a length of 0.24λ. The dipole elements were oriented along the Y-axis in the XY-plane containing the array. The beamwidth of the short dipole element was found to be 85.2° in the YZ-plane, while it has omnidirectional pattern in the XZ-plane, as shown in Fig. 12. For the given array dimensions and the area of interest in the focal plane, the short dipole can adequately represent the isotropic sources used in the MATLAB simulation. Fig. 13 compares the results of the total field E_t at the point $P(0, 0, z)$ obtained from the MATLAB and CST simulations. Fig. 14 shows the variations of the electric field E_t at the point $P(x, y, F)$ on the focal plane obtained from the MATLAB and CST simulations. Good agreement between the results obtained from the CST and MATLAB simulations can be seen, especially in the region around the focus. The minor differences that are away from the focal region can be attributed to the use of short dipole elements instead of isotropic sources. In those regions the radiation pattern of the short-dipole starts to influence the magnitude of the field radiated by the various elements of the array.

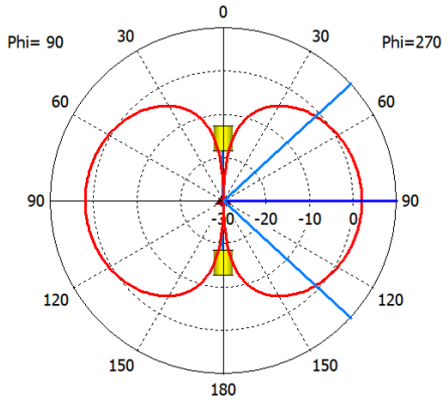

Figure 12. The radiation pattern of the short dipole in the YZ-plane.

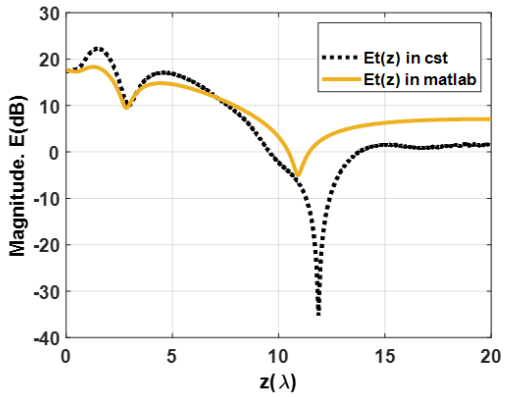

Figure 13. Variation of the magnitude of the total field $E_t(z)$ of the proposed array at the observation point $P(0, 0, z)$, obtained from the MATLAB and the CST simulations. $F = 5\lambda$, inner elements = 4, outer elements = 10.

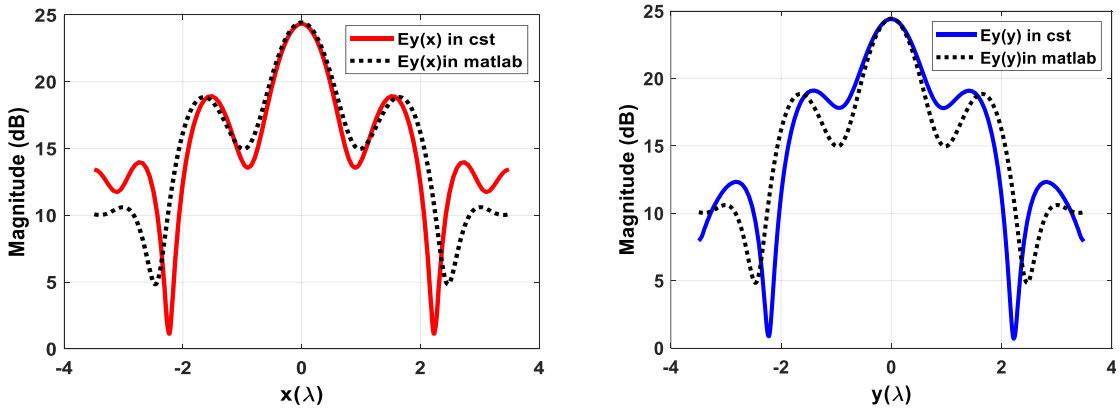

Figure 14. Variation of the electric field E_t at an observation point $P(x, y, F)$ on the focal plane ($z = F$) obtained from the MATLAB and the CST simulations. (a) Variation along X-axis, $E_t(x)$. (b) Variation along Y-axis, $E_t(y)$.

6. CONCLUSIONS

The focusing properties of a proposed circular array composed of elements placed on two concentric circular rings have been demonstrated. The radii of the two rings are designed such that the distances from the elements on the outer ring to the focal point are made larger by one wavelength than those on the inner ring. Thus, the contributions of the elements of the two rings add constructively at the focal point, and destructively elsewhere. There is no need for a phase shifter, and thus, this is a favorable property compared to square focused array having $N \times N$ elements, which requires $N^2/4$ phase shifters. The performance parameters, such as the field distribution around the focal point, the level of the field at the focal point, the depth of field, and the shift in the position of the focus for the proposed array, showed favorable properties. Another simulation using the CST microwave suit verified the results obtained from the simulations on the MATLAB program. The results obtained for the concentric circular array are useful to help solve the problems of hyperthermia and imaging applications.

REFERENCES

1. Bogosanovic, M. and A. G. Williamson, "Microstrip antenna array with a beam focused in the near-field zone for application in noncontact microwave industrial inspection," *IEEE Transactions on Instrumentation and Measurement*, Vol. 56, No. 6, 2186–2195, 2007.
2. Daniels, D. J., *Ground Penetrating Radar*, IET, London, United Kingdom, 2004.
3. Nepa, P., A. Buffi, A. Michel, and G. Manara, "Technologies for near-field focused microwave antennas," *International Journal of Antennas and Propagation*, Vol. 2017, Article ID 7694281, 2017.
4. Guo, T. C., W. W. Guo, and L. E. Larsen, "A local field study of a water-immersed microwave antenna array for medical imagery and therapy," *IEEE Transactions on Microwave Theory and Techniques*, Vol. 32, 844–854, 1984.
5. Lee, K., J.-Y. Kim, and S.-H. Son, "Experimental phantom test of 925 MHz microwave energy focusing for non-invasive local thermotherapy," *Results in Physics*, Vol. 38, No. 105585, 2022.
6. Nepa, P. and A. Buffi, "Near-field focused microwave antennas near-field shaping and implementation," *IEEE Antennas & Propagation Magazine*, Vol. 59, No. 3, 42–53, 2017.
7. Ismail, M. S. and K. H. Sayidmarie, "Investigation of three array geometries for focused array hyperthermia," *The International Symposium on Antennas and Propagation*, Sapporo, Japan, 1992.
8. Sayidmarie, K. H. and A. M. Abdulkhaleq, "Investigation of six array geometries for focused array hyperthermia applications," *Progress In Electromagnetics Research M*, Vol. 23, 181–194, 2012.
9. Tomás, J. J., M. Arrebola, G. León, and F. Las-Heras, "Near-field focussed array with two simultaneous and independent spots," *Proceedings of the 2012 IEEE International Symposium on Antennas and Propagation*, 1–2, Chicago, IL, USA, 2012.
10. Chou, H. T., M. R. Pino, P. Nepa, and C. Y. Liu, "Near-field focused subarrays in a multi-panel configuration," *IEEE Access*, Vol. 7, 143097–143108, 2019.
11. Cheng, Y. J. and F. Xue, "Ka-band near-field-focused array antenna with variable focal point," *IEEE Transactions on Antennas and Propagation*, Vol. 64, No. 5, 1725–1732, 2016.
12. Ayestarán, R. G., "Fast near-field multifocusing of antenna arrays including element coupling using neural networks," *IEEE Antennas and Wireless Propagation Letters*, Vol. 17, No. 7, 1233–1237, 2018.
13. Yi, X., X. Chen, L. Zhou, and S. Hao, "A high-efficiency near-field focused transmitting antenna based on the equal power divisions," *AIP Advances*, Vol. 10, No. 11, 115111, 2020.
14. Sayidmarie, K. H. and Eanaas U. Taha, "Development of a semi-circle phased array for local hyperthermia," *2005 IEEE International Symposium on Microwave, Antenna, Propagation and EMC Technologies for Wireless Communications Proceedings*, 1430–1434, 2005.
15. Alkhalifeh, K., R. Sarkis, and C. Craeye, "Design of a novel 3D circular Vivaldi antennas array for ultra-wideband near-field radar imaging," *2012 6th European Conference on Antennas and Propagation (EUCAP)*, 898–901, Prague, Czech Republic, 2012.
16. Siragusa, R., P. Lemaitre-Auger, and S. Tedjini, "Near field focusing circular microstrip antenna array for RFID applications," *IEEE Antennas and Propagation Society International Symposium*, 1–4, 2009.
17. Gowda, V. R., M. F. Imani, T. Sleasman, O. Yurduseven, and D. R. Smith, "Focusing microwaves in the fresnel zone with a cavity-backed holographic metasurface," *IEEE Access*, Vol. 6, 12815–12824, 2018, doi: 10.1109/ACCESS.2018.2802379.
18. Huang, R., B. Liu, and Q. Tan, "A near-field focused circular array based on dielectric resonator antenna," *IEEE International Symposium on Antennas and Propagation and USNC-URSI Radio Science Meeting (APS/URSI)*, 4–10, Dec. 2021.
19. Han, X., S. Ding, Y. Huang, Y. Zhou, H. Tang, and B. Wang, "Frequency diversity array for near-field focusing," *Electronics*, Vol. 9, 958, 2020, doi: 10.3390/electronics9060958.
20. Balanis, C. A., *Antenna Theory Analysis and Design*, John Wiley & Sons. Inc., New York, 2005.